BIBECHANA
Vol. 22, No. 2, August 2025, 188-195

ISSN 2091-0762 (Print), 2382-5340 (Online)
Journal homepage: http://nepjol.info/index.php/BIBECHANA
Publisher:Dept. of Phys., Mahendra Morang A. M. Campus (Tribhuvan University)Biratnagar

First Principles Calculations of Mechanical, Electronic, Thermoelectric and Thermal Properties of ZnCu

Shashit Kumar Yadav*, Subash Dahal, Bhupal Guragain ,
Department of Physics, Mahendra Morang Adarsh Multiple Campus

Tribhuvan University,Biratnagar, Nepal
*Corresponding author. Email: sashit.yadav@mmamc.tu.edu.np

Abstract

The structural, mechanical, electronic and thermoelectric properties of ZnCu were investigated using Density Functional Theory (DFT). The Perdew–Burke–Ernzerhof (PBE) exchange-correlation functional within the Generalized Gradient Approximation (GGA) was employed in the Quantum ESPRESSO package for the purpose. The ZnCu compound was found to be both mechanically and dynamically stable. Analysis of its elastic and electronic properties reveals that ZnCu is mechanically stable, anisotropic, and exhibits metallic behavior. Furthermore, thermoelectric property analysis indicates that ZnCu achieves its highest power factor at 300 K. The study of thermodynamic properties suggests that ZnCu retains mechanical stability at elevated temperatures.

Keywords

ZnCu compound, Quantum Espresso, electronic properties, phonon, thermoelectric properties.

Article information

Manuscript received: January 10, 2025; Revised: April 12, 2025; Accepted: May 26, 2025
DOI https://doi.org/10.3126/bibechana.v22i2.79223

1 Introduction

Alloying materials serve an important role in improving the qualities of materials for a variety of applications by increasing their strength, durability, and corrosion resistance. The material can be alloyed to achieve the qualities that alloy components lack for practical application [1]. There are enormous possibilities for alloying the material, but copper alloy has gained its own importance in the fields of machinery, electrical industry, and construction over the past year [2, 3]. Among the different possible alloys of copper, the ZnCu alloy stands out due to its potential application in diverse domains. The unique combination of zinc and copper provides promising characteristics [4–8].

Different research has been conducted to study the properties of the ZnCu alloy. For example, Iwaoka and Hirosawa used first principles method to calculate elastic properties of three different complex of Cu-Zn system to improve the stiffness of aluminum alloy [4]. Similarly, Liu et al. studied the structural, elastic, and electronic properties of Cu-X (X = Al, Be, Mg, Sn, Zn, and Zr) by the first-principles calculations [8]. Furthermore, Tang et al. used a modified quasi-chemical model (MQM) to describe the Gibbs energy of the liquid phase [9].

Despite significant progress in material science, comprehensive studies that integrate structural, electronic, elastic, thermoelectric, and thermal properties of ZnCu crystal structure are still sparse. Therefore, this work attempts to explain these properties of the ZnCu compound using the first principles calculations employing Quantum Espresso codes [10].

2 Computational Details

The first principles calculation of ZnCu structure was performed using the Quantum Espresso software package [10]. The crystal structure was first optimized by performing the VC-relax calculation using Perdew-Burke-Ernzerhof (PBE) of scalar relativistic exchange-correlation functional and ionic potentials described by ultrasoft pseudopotential (USPP) for Zn and Cu downloaded from the material cloud website [11]. The plane wave cutoff energy was set to 40 Ry and 320 Ry was set for the wave function and charge density. The Brillouin zone was determined using Monkhorst-Pack for self-consistent field calculation and for density of state (DOS) calculation. The electronic band structure was calculated along the high-symmetry point in the Brillouin zone using the path $\Gamma - X - M - \Gamma - R - X|R - M$.

The bulk modulus was calculated using the Murnaghan equation of state using the ev.x utility of Quantum Espresso [12]. Furthermore, the `Thermo_pw` [13] postprocessing tool was used to calculate the elastic constant, which allowed for the calculation of mechanical properties such as bulk modulus, young modulus, shear modulus, and Poisson ratio of the material. Electronic transport properties were calculated with the help of the Boltztrap code [12, 14]. The output information of non-self-consistent field calculation was used as input for boltztrap software, which solves the Boltzmann transport equation to determine electrical conductivity, Seebeck coefficient, and thermal conductivity. The phonon calculation was executed in the Phonopy package [15] using the finite displacement method on a supercell. Finally, thermal properties such as heat capacity at constant volume, free energy, and entropy were calculated.

3 Results and Discussion

3.1 Structural properties

Figure 1 shows the ZnCu crystal structure which is a tetraauricupride cubic structure in space group $Pm\bar{3}m$ with all bond lengths of 2.53 Å. Zn is bonded with eight Cu atoms in body centered geometry [16].

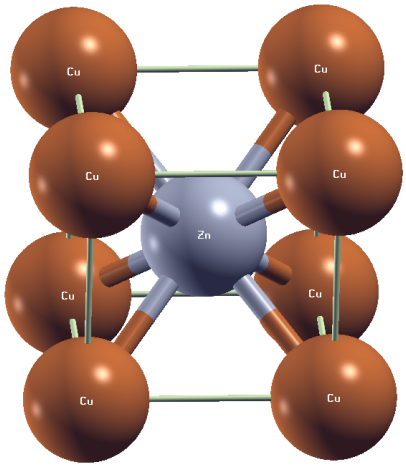

Figure 1: Crystal structure of ZnCu.

Using the first principles calculations in Quantum Espresso software, the total energies were minimized as a function of the lattice parameter for the material. The lattice parameter (a), bulk modulus ($B_0 = -V\frac{\partial P}{\partial V}$), and pressure derivative (B') of the ZnCu crystal structure are derived by fitting the Murnaghan equation of state as [17]

$$P(V) = \frac{B_0}{B'}\left[\left(\frac{V_0}{V}\right)^{B'} - 1\right] \quad (1)$$

where V_0 is the equilibrium volume and $B' = dB/dP$.

The Murnaghan equation of state is fitted using the `ev.x` tool of Quantum Espresso to calculate total energy as a function of unit cell volume. The obtained value of the lattice parameter is 2.96628 Å, which is consistent with the experimental value of 2.959 Å [4]. Similarly, bulk modulus (B_0) and its pressure derivative (B') are found to be 115.00 GPa and 5.02, respectively. The obtained value of bulk modulus is in good agreement with the value in the materials project database, which is 116.00 GPa [18]; validating the present computational approaches.

3.2 Vibrational properties

The phonon serves as a medium for understanding transmission of vibrational energy in the material. Utilizing the `phonopy` algorithm [15], the phonon frequency of ZnCu was calculated. A $2\times2\times2$ supercell was created to collect force sets for analyzing the phonon band structures and phonon density of states (DOS). The phonon dispersion curves and the corresponding phonon density of states (DOS) of ZnCu are shown in Figure 2. These calculations

were performed to assess the dynamical stability and lattice vibrational behavior of the compound.

The phonon dispersion curve displays the vibrational frequencies along high-symmetry directions in the Brillouin zone. Importantly, no imaginary frequencies (i.e., frequencies below zero) are observed throughout the entire Brillouin zone, indicating that the ZnCu structure is dynamically stable in its equilibrium configuration. The phonon spectrum features both acoustic and optical branches. The acoustic modes originate from the Γ- point and extend up to about 4 THz, while the optical modes span from about 4 THz to over 6.5 THz. The separation between the acoustic and optical branches suggests a moderate mass difference between Zn and Cu atoms and indicates potential phonon scattering behavior relevant to thermal transport. The phonon density of state (DOS) exhibits multiple sharp peaks, especially in the high-frequency region (4–7 THz), corresponding to localized optical modes. The lower-frequency region shows a more gradual increase in DOS, associated with acoustic phonons. This distribution of vibrational states implies that optical phonons significantly contribute to the vibrational properties, while acoustic phonons dominate low-temperature specific heat and thermal conductivity. he phonon DOS achieved is consistent with the findings of a previous study by Peter et al. for β-ZnCu [7].

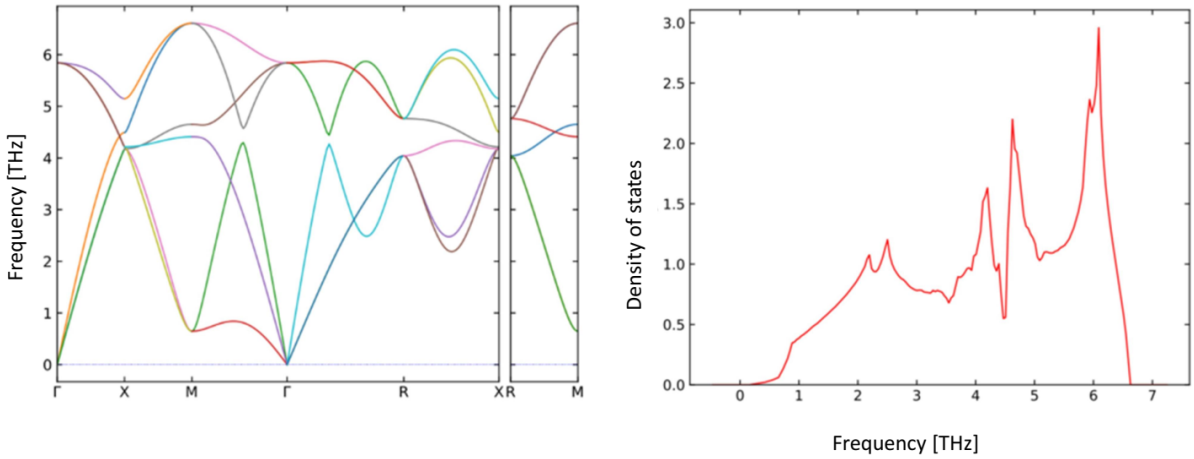

Figure 2: Phonon band structures and phonon DOS of ZnCu.

3.3 Elastic properties

The elastic constant matrices (C_{ij}) were calculated using `Thermo_pw` utility of Quantum Espresso. Three independent elastic constants; C_{11}, C_{12}, and C_{44} for cubic structure of ZnCu were obtained. These elastic constants were further used to calculate the elastic property through Voigt–Reuss–Hill (VRH) methods [19–22]. The relation of shear modulus (G) and bulk modulus (B) are expressed as [12, 19, 23]

$$G_V = \frac{C_{11} - C_{12} + 3C_{44}}{5} \tag{2}$$

$$G_R = \frac{5C_{44}(C_{11} + C_{12})}{4C_{44} + 3(C_{11} - C_{12})} \tag{3}$$

$$G = \frac{G_V + G_R}{2} \tag{4}$$

$$B_V = B_R = \frac{C_{11} + 2C_{12}}{3} \tag{5}$$

$$B = \frac{B_V + B_R}{2} \tag{6}$$

Similarly, Young's modulus (Y), Poisson's ratio (ν), and universal elastic anisotropy index (A^U) can be calculated using the relations as [19, 20, 23]

$$Y = \frac{9BG}{3B + G} \tag{7}$$

$$\nu = \frac{3B - 2G}{2(3B + G)} \tag{8}$$

$$A^U = 5\left(\frac{G_V}{G_R}\right) + \left(\frac{B_V}{B_R}\right) - 6 \tag{9}$$

Table 1 shows the calculated values of these elastic parameters. Born criteria for mechanical stability of the cubic system, i.e., $C_{11} > 0$, $C_{44} \geq 0$, $C_{11} \geq |C_{12}|$ and $C_{11} + 2C_{12} \geq 0$ are satisfied by the calculated value of elastic constants [12, 22, 23]. This shows that ZnCu crystal is mechanically stable. Furthermore, the value of bulk modulus (B_0) calculated using Murnaghan equation of state in the Section 3.1 and Voigt-Reuss-Hill methods using Equation (3.3) are comparable with the value predicted in the material project database [18] and ref.

[4]. The small discrepancy in the calculated values of elastic parameters with material project database may be due to the use of different pseudopotentials. We have used PBE type pseudopotential whereas the later, ref. [18], have used PBESol type pseudopotential.

Table 1: Calculated values of elastic parameters for ZnCu complex

Parameter	This work	Material project [18]	Other [4]
C_{11} (GPa)	152.692	134.8	–
C_{12} (GPa)	102.697	104.7	–
C_{44} (GPa)	96.992	75.4	–
B (GPa)	119.362	116	117.4
G (GPa)	56.632	46	40.1
Y (GPa)	145.975	107.7	–
ν	0.295	0.33	0.34
A^U	2.565	3.57	3.87

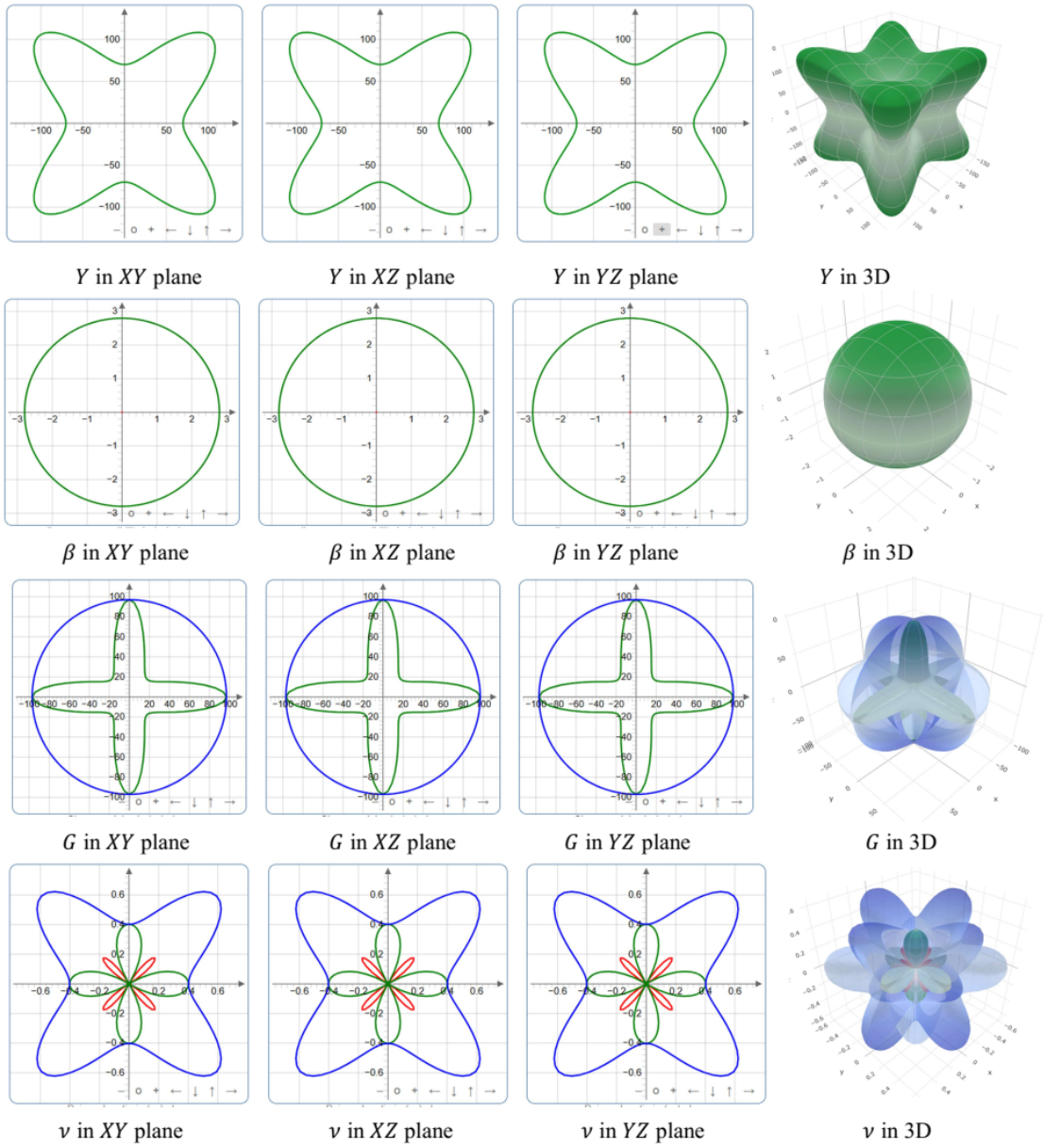

Figure 3: Spatial dependence and 3D visualization of Young's Modulus (Y), linear compressibility (β), shear modulus (G) and Poisson's ratio (ν) of ZnCu.

The bulk modulus (B) characterizes the material's resistance to uniform compression and is intrinsically linked to its crystal structure, including the nature and length of chemical bonds . The shear modulus (G), or modulus of rigidity, quantifies the material's response to shear stress, reflecting its ability to resist deformation caused by tangential forces that induce relative motion between adjacent atomic layers. Young's modulus (Y) represents the stiffness of the material under uniaxial tensile stress and provides a comprehensive measure of its elastic rigidity [16, 24, 25]. Its higher values indicate greater resistance to deformation. The calculated value of $Y = 145.975$ GPa, indicating moderately high stiffness, consistent with metallic bonding.

Additional mechanical parameters derived from the elastic moduli, namely Pugh's ratio ($k = B/G$), Poisson's ratio (ν), and the universal anisotropy index (A^U) offer valuable insight into the bonding characteristics, mechanical behavior, and elastic anisotropy of crystalline materials [26]. According to Pugh's criterion, materials with $k > 1.75$a re typically classified as brittle, while those with $k > 1.75$ are considered ductile [19]. The calculated value of $k = 2.11$, indicating the material to be ductile. The calculated value of $\nu = 0.295$ corresponding that the material exhibits metallic ductility, as predicted by k. Furthermore, a universal anisotropy index of $A^U = 1$ denotes a mechanically isotropic material, whereas any deviation from this value indicates the presence of elastic anisotropy [19]. The obtained value of $A^U = 2.565$ corresponding that te material to be significantly anisotropic, which may affects its mechanical behaviour under directional stress.

The directiona dependence of the elastic properties was also analyzed using the ELATE software [27], which processes the second-order elastic constants (C_{ij}) in Voigt notation. Based on the calculated values of C_{11}, C_{12} and C_{44}, Table 1. The software then generated 2D and 3D plots of mechanical properties, including Young's modulus (Y), linear compressibility β, shear modulus (G) and Poisson's ratio (ν). The obtained results are summarized in Table 2, and their 2D and 3D plots are visualized in Figure 3. The uniform shapes of the respective plots indicate isotropy, while deviations reflect elastic nisotropy.

The software utilizes distinct color schemes to represent elastic properties in 2D and 3D visualizations [27]. For Y and β, green indicates positive values and red denotes negative values. In the case of G and ν, up to three colors are employed: solid green and translucent blue for positive values, and translucent red for negative values, particularly relevant for Poisson's ratio, which may become negative in specific crystallographic directions. It can be observed that the spatial dependence of Y, β and G are found to be positive for the material with finite and non-negative values of respective anisotropy. Figure 3. But the value of ν is found to be negative (there is presence of red colour) with infinite value of anisotropy indicating its directional dependence.

Table 2: Variations of Young's modulus (Y), linear compressibility (β), shear modulus (G), and Poisson's ratio (ν), along with their corresponding anisotropy ratios for ZnCu

Parameter	Y **(GPa)**		β (TPa^{-1})		G **(GPa)**		ν	
	Min	Max	Min	Max	Min	Max	Min	Max
Value	70.009	228.960	2.7926	2.7926	24.998	96.992	-0.24656	0.83841
Anisotropy	3.266		1.000		3.880		∞	

3.4 Electronic properties

The electronic properties of the material were investigated using DFT within the PBE scalar relativistic approximation. The calculated electronic band structures, density of states (DOS), and partial density of states (PDOS) are presented in Figure 4(a,b).

The band structures of te material shows multiple bands crossing the Fermi level (E_F), consistent with its metallic character, as shown in Figure 4(a). Notably, several highly dispersive bands are observed near E_F along the Γ-X, R-X, and M–Γ directions, indicating the presence of high carrier mobility in these directions. In contrast, the presence of relatively flat bands around -3 eV to -2 eV corresponds to localized Cu-d states, as supported by the PDOS in Figure 4(b). The absence of a band gap and the significant overlap of conduction and valence bands near E_F suggest that ZnCu can exhibit good electrical conductivity. The availability of partially filled conduction states also implies the possibility of tuning thermoelectric performance through appropriate doping or carrier concentration adjustment.

The PDOS plot reveals that the Cu-3d orbitals dominate the valence region, particularly within the energy range from approximately -4 eV to -2 eV,

as shown in Figure 4(b). The Zn-3d states contribute mainly at deeper energies (−6 eV to −3 eV), whereas the s and p orbitals of both Zn and Cu exhibit relatively minor contributions. The non-zero density of states at the Fermi level confirms the metallic nature of ZnCu, which further supports the results of band structures.

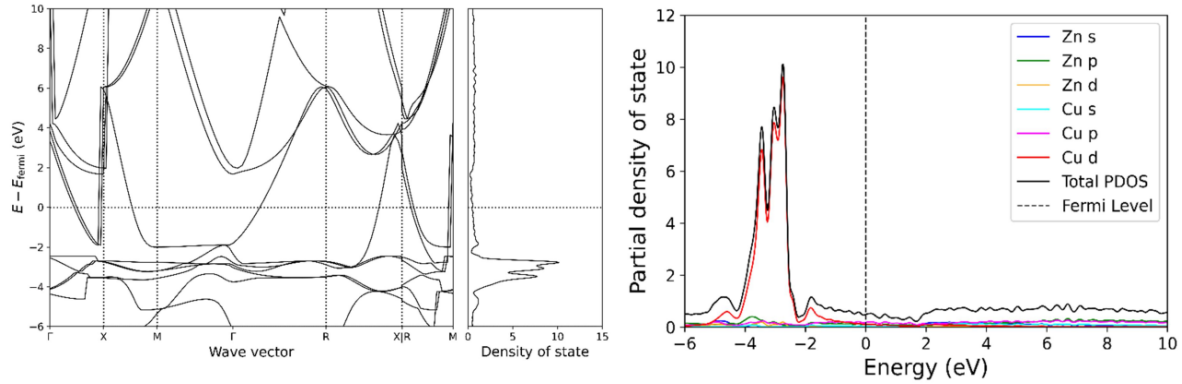

Figure 4: Electronic band structures, density of states and partial density of states (PDOS) of ZnCu.

3.5 Thermoelectric properties

The thermoelectric properties of the ZnCu were investigated using Boltzmann transport equation implemented in BoltzTrap2 codes [12, 14]. The calculations were basically focusing on the Seebeck coefficient (S), electrical conductivity (σ/τ_0), thermal conductivity (k_e/τ_0), and power factor ($PF = S^2\sigma/\tau$). The calculated values of these parameters are plotted as a function of temperature in Figure 5.

The Seebeck coefficient exhibits a nonlinear trend, starts slightly positive from about 200 K and becomes strongly negative around/at 300 K. With further increase in the temperature of the sample, plot of Seebeck coefficient gradually increases towards zero as temperature approaches 850 K. The change in sign of the coefficient indicates a crossover in carrier type dominance. Its positive value indictes hole-like or p-type behaviour whereas negative value indicates electron-like or n-type behaviour. The sharp negative peak suggests dominant n-type conduction at intermediate temperatures.

The plot of electrical conductivity decreases with temperature (top right panel of Figure 5). This behaviour is expected for metallic semiconducting materials, in which increased phonon scattering takes place at higher temperatures thereby reducing the conductivity of material. Further, the thermal conductivity of the material increases linearly with temperature (bottom left panel of Figure 5). This behaviour is typical as thermal conductivity due to electrons generally increases with temperature in metallic system.

The power factor combines Seebeck and conductivity, which is a key quantity in thermoelectric performance. The plot of power factor stars from zero at/about 200 K and then gradually increases attaining peak value around 300 K. It decreases sharply then after with further increase in temperature (bottom right panel of Figure 5). The peak near 300 K indicates optimal thermoelectric performance at room temperature.

4 Conclusions

The structural, mechanical, electronic, and thermoelectric properties of ZnCu have been systematically investigated using the first principles calculations employing Quantum Espresso codes. Elastic constant calculations confirm the mechanical stability of the compound, satisfying the Born stability criteria for cubic systems. Pugh's ratio and Poisson's ratio indicate that ZnCu is ductile, while the universal anisotropy index and ELATE visualizations reveal significant elastic anisotropy. Electronic band structure analysis demonstrates that ZnCu exhibits metallic behavior, with no band gap across the Fermi level. This metallic nature supports good electrical conductivity, which is a critical factor in thermoelectric performance. Thermoelectric calculations show that ZnCu achieves its highest power factor at 300 K, highlighting its potential for energy conversion applications. Thus, ZnCu

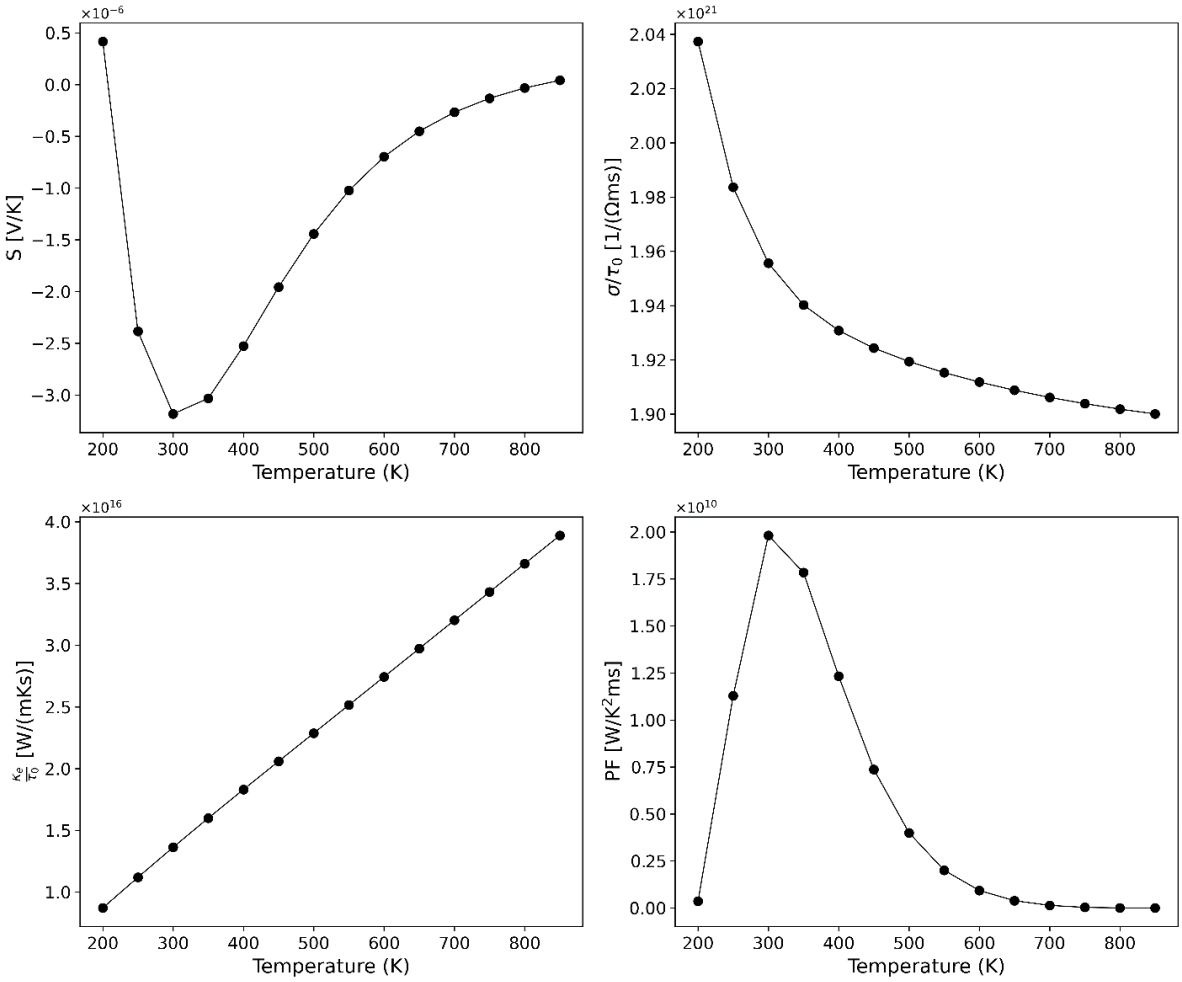

Figure 5: Temperature dependence of Seebeck coefficient (S), electrical conductivity (σ/τ_0), thermal conductivity (k_e/τ_0), and power factor ($PF = S^2\sigma/\tau$) of ZnCu.

combines mechanical robustness, metallic conductivity, and promising thermoelectric performance, making it a potential candidate for multifunctional applications in structural and energy-related technologies.

References

[1] Sah D, Adhikari D, Yadav S. Temperature-Dependence of Mixing Properties of Cu-Ti Liquid Alloy. Adhyayan Journal. 2023;10(10):1–10.

[2] Yadav S, Gautam M, Adhikari D. Mixing properties of Cu–Mg liquid alloy. AIP Advances. 2020;10(12).

[3] Godbole R, Jha S, Milanarun M, Mishra A. Thermodynamics of liquid Cu–Mg alloys. Journal of alloys and compounds. 2004;363(1-2):187–193.

[4] Iwaoka H, Hirosawa S. First-principles calculation of elastic properties of Cu-Zn intermetallic compounds for improving the stiffness of aluminum alloys. Computational Materials Science. 2020;174:109479.

[5] Liu Q, Cheng L. Structural evolution and electronic properties of Cu-Zn alloy clusters. Journal of Alloys and Compounds. 2019;771:762–768.

[6] Li L, zhou Wang Y, Liu Q, Wang K, Bao Y, Zhao B, et al. The thermodynamic properties of disorder CuZn solid solution and nonstoichiometric Cu-Zn alloy: Pseudo-atomic lattice inversion potential method. Journal of Solid State Chemistry. 2020;289:121488.

[7] Peter M, Potzel W, Steiner M, Schäfer C, Karzel H, Schiessl W, et al. Lattice-dynamical effects and hyperfine interactions in Cu-Zn alloys. Physical Review B. 1993;47(2):753.

[8] Liu Y, Wang J, Gao Qn, Du Y. Structural, elastic and electronic properties of Cu-X compounds from first-principles calcula-

tions. Journal of Central South University. 2015;22(5):1585–1594.

[9] Tang Y, Ma J, Han D, Wang J, Qi H, Jin L. Critical evaluation and thermodynamic optimization of the Cu-Zn, Cu-Se and Zn-Se binary systems. Metals. 2022;12(9):1401.

[10] Giannozzi P, Baroni S, Bonini N, Calandra M, Car R, Cavazzoni C, et al. QUANTUM ESPRESSO: a modular and open-source software project for quantumsimulations of materials. Journal of physics: Condensed matter. 2009;21(39):395502.

[11] Talirz L, Kumbhar S, Passaro E, Yakutovich AV, Granata V, Gargiulo F, et al. Materials Cloud, a platform for open computational science. Scientific data. 2020;7(1):299.

[12] Yadav S, Dahal S, Khadka R, Guragain B, Pokharel P, Oli P, et al. First Principles Study of Electronic, Vibrational, Elastic, and Thermodynamic Properties of Sc-X (X= P, S, Se) Compounds. Engineering Reports. 2025;7(1):e13115.

[13] Dal Corso A. Elastic constants of beryllium: a first-principles investigation. Journal of Physics: Condensed Matter. 2016;28(7):075401.

[14] Madsen GK, Singh DJ. BoltzTraP. A code for calculating band-structure dependent quantities. Computer Physics Communications. 2006;175(1):67–71.

[15] Togo A, Chaput L, Tadano T, Tanaka I. Implementation strategies in phonopy and phono3py. Journal of Physics: Condensed Matter. 2023;35(35):353001.

[16] Jain A, Ong SP, Hautier G, Chen W, Richards WD, Dacek S, et al. Commentary: The Materials Project: A materials genome approach to accelerating materials innovation. APL materials. 2013;1(1).

[17] Bhardwaj P, Singh S. First principle calculation of structural, electronic and elastic properties of rare earth nitride. Mater Sci-Poland. 2016;34(4):715.

[18] Project M. mp-987: Material Properties; 2025. Accessed: 2025-05-27. Available from: https://next-gen.materialsproject.org/materials/mp-987.

[19] Pokharel P, Yadav S, Pantha N, Adhikari D. Strain-dependent electronic, mechanical and piezoelectric properties of ZrSiO3 2D monolayer: A first principle approach. Journal of Physics and Chemistry of Solids. 2024;193:112198.

[20] Pokharel P, Yadav SK, Pantha N, Sharma B, Adhikari D. Structural, electronic, optical, magnetic, and mechanical properties of SmMnO3 perovskite with europium and yttrium doping: A first-principles study. AIP Advances. 2024;14(12).

[21] Gupta PC, Adhikari R. Structural, Elastic, Electronic and Optical Properties of $Be\_2X(X = C, Si, Ge, Sn)$: First Principle Study. arXiv preprint arXiv:211210521. 2021;.

[22] Chaudhary U, Chaudhary S, Yadav DK, Kaphle GC, Yadav SK. First-Principles Investigation of Structural, Elastic, Electronic, and Optical Properties of AcMO3 (M= B, Sc) Perovskites. physica status solidi (b). 2025;262(5):2400574.

[23] Gao J, Liu QJ, Tang B. Elastic stability criteria of seven crystal systems and their application under pressure: Taking carbon as an example. Journal of Applied Physics. 2023;133(13).

[24] Cao Y, Zhu J, Liu Y, Nong Z, Lai Z. First-principles studies of the structural, elastic, electronic and thermal properties of Ni_3Si. Computational Materials Science. 2013;69:40–45.

[25] Hadi MA, Christopoulos SR, Chroneos A, Naqib SH, Islam AKMA. DFT insights into the electronic structure, mechanical behaviour, lattice dynamics and defect processes in the first Sc-based MAX phase Sc_2SnC. Scientific Reports. 2022;12(1):14037.

[26] Jamal M, Asadabadi SJ, Ahmad I, Aliabad HR. Elastic constants of cubic crystals. Computational Materials Science. 2014;95:592–599.

[27] Gaillac R, Pullumbi P, Coudert FX. ELATE: An open-source online application for analysis and visualization of elastic tensors. Journal of Physics: Condensed Matter. 2016;28(27):275201.